Energy Transfer in the Peridinin-Chlorophyll Protein Complex Reconstituted with Mixed Chlorophyll Sites

Tomáš Polívka,*† Torbjörn Pascher,‡ and Roger G. Hiller§

*Institute of Physical Biology, University of South Bohemia, Czech Republic; †Institute of Plant Molecular Biology, Biological Centre, Czech Academy of Sciences, Czech Republic; ‡Department of Chemical Physics, Lund University, Sweden; and §Department of Biological Sciences, Macquarie University, NSW, Australia 2109

ABSTRACT We use femtosecond transient absorption spectroscopy to study chlorophyll (Chl)-Chl energy transfer in the peridinin-chlorophyll protein (PCP) reconstituted with mixtures of either chlorophyll *b* (Chl*b*) and Chl*d* or Chl*a* and bacteriochlorophyll *a* (BChl*a*). Analysis of absorption and transient absorption spectra demonstrated that reconstitution with chlorophyll mixtures produces a significant fraction of PCP complexes that contains a different Chl in each domain of the PCP monomer. The data also suggest that binding affinity of Chl*a* is less than that of the other three Chl species. By exciting the Chl species lying at higher energy, we obtained energy transfer times of 40 ± 5 ps (Chl*b*-Chl*d*) and 59 ± 3 ps (Chl*a*-BChl*a*). The experimental values match those obtained from the Förster equation, 36 and 50 ps, respectively, showing that energy transfer proceeds via the Förster mechanism. Excitation of peridinin in the PCP complex reconstituted with Chl*a*/BChl*a* mixture provided time constants of 2.6 and 0.4 ps for the peridinin-Chl*a* and peridinin-BChl*a* energy transfer, matching those obtained from studies of PCP complexes reconstituted with single chlorophyll species.

INTRODUCTION

Photosynthetic performance of all organisms relies on the efficiency of their antenna complexes, which capture sunlight in the form of excitation energy. This excitation energy is transferred to the reaction center where the charge separation takes place. Although only two types of reaction centers are found in the vast diversity of photosynthetic organisms, the variability of antenna complexes is considerable, reflecting different light-harvesting strategies (1). Cyanobacteria and cryptophytes use extrinsic water-soluble phycobilins whose chromophores are linear tetrapyrroles (2). Most membrane-intrinsic antenna complexes utilize (bacterio)chlorophylls ((B)Chl) as major light-harvesting pigments, with carotenoids as supporting pigments covering the spectral region not accessible to (B)Chl (1,3–6). The water soluble light-harvesting complex of dinoflagellates, peridinin-chlorophyll protein (PCP), is remarkable in using the relatively polar carotenoid peridinin as its main chromophore (7,8). PCP isolated from *Amphidinium carterae* contains eight peridinins and two Chl*a* molecules in each monomer. Its structure, determined to 2.0 Å resolution, reveals that the pigments are arranged as two very similar clusters of four peridinin and one Chl*a* molecules (9).

The detailed structural knowledge and unique pigment composition of PCP has become a basis for numerous experimental and theoretical studies of energy transfer pathways within the PCP complex carried out in the past decade (see Polívka et al. (8) for a review). These studies demonstrated that energy transfer from peridinin to Chl*a* occurs with nearly 90% efficiency (7,10–12). Peridinin contains a conjugated carbonyl group that induces an intramolecular charge transfer (ICT) state into the peridinin excited state manifold (13–16). Though the details of coupling between the S_1 and ICT states are still unclear and in PCP these two states are assumed to act as one state denoted S_1/ICT (15–18), the major effect of the ICT state is to make the peridinin excited state dynamics dependent on polarity of the environment (13–18). Because the dominating peridinin-Chl*a* energy transfer pathway in PCP occurs via the S_1/ICT state (7,10–12), it was hypothesized that tuning the polarity of the immediate environment of peridinin molecules may be an important factor enhancing the overall efficiency of peridinin-Chl*a* energy transfer (11,19). The importance of the polarity-induced activation of the ICT state for carotenoid-Chl energy transfer was also shown in other light-harvesting complexes utilizing peridinin or other carbonyl carotenoids. The ICT state actively participates in energy transfer in the intrinsic light-harvesting complex of *A. carterae* (20), the fucoxanthin-chlorophyll protein from the diatom *Cyclotella meneghiniana* (21), or even artificial light harvesting antenna utilizing peridinin and fucoxanthin (22).

Besides the peridinin-Chl*a* energy transfer, other studies focused on energy transfer between the two Chl*a* molecules located in separate domains of the PCP monomer. At room temperature, these Chl*a* molecules have slightly different energies (23,24). Fluorescence anisotropy decays monitoring Chl-Chl energy transfer within the PCP monomer are characterized by a time constant of 6 ps that can be successfully modeled by the Förster energy transfer mechanism (25). Essentially the same time constant was obtained from transient absorption data recorded at 20 K (26,27). A discovery of a new PCP form, the so-called high-salt PCP (HSPCP) promoted further studies of Chl-Chl energy transfer. The HSPCP complex exhibits a clear splitting of the Q_y bands of Chl*a* at low temperature

Submitted October 6, 2007, and accepted for publication December 4, 2007.

Address reprint requests to Tomáš Polívka, Institute of Physical Biology, University of South Bohemia, Zamek 136, CZ-373 33 Nove Hrady, Czech Republic. E-mail: polivka@ufb.jcu.cz.

Editor: Klaus Schulten.

0006-3495/08/04/3198/10 $2.00

doi: 10.1529/biophysj.107.123430

(26,27). Assuming the Förster mechanism, the splitting of the Q_y bands leads to a decrease of spectral overlap between donor emission and acceptor absorption, resulting in a 23 ps time constant for Chl-Chl energy transfer (27). In addition to the change in spectral overlap, the ~4 times slower energy transfer in the HSPCP is also caused by a weaker Chl-Chl interaction because the Chl-Chl distance in HSPCP is slightly longer than in PCP ((27), and T. Schulte, F. P. Sharples, R. G. Hiller, and E. Hofmann, unpublished. Coordinates have been deposited in the Protein Data Bank under ID 2C9E.).

A promising method for studying mechanisms of energy transfer is reconstitution of light-harvesting complexes with different pigments (29). This method has been successfully used to monitor spectral overlap dependence of energy transfer between B800 and B850 BChl*a* molecules in the LH2 antenna complex of purple bacteria (30). It has also been used to investigate pigment binding sites and energy transfer in many LHCPs from plants (31). Recent reconstitution of the PCP complexes with heterologously expressed apoprotein and peridinin together with a series of chlorophylls (Chl*b*, Chl*a*, acetyl-Chl*a*, Chl*d*, and BChl*a*) having various positions of their Q_y bands (32) offered another possibility for testing the mechanisms of energy transfer in the PCP complex. Polívka et al. studied dependence of peridinin-Chl energy transfer rate on the position of the Q_y band of the Chl acceptor, showing that the S_1/ICT-Q_y energy transfer rate can be successfully modeled by the Förster mechanism. Interestingly, for chlorophylls having red-shifted Q_y band as compared with the Chl*a*, the peridinin-Chl energy transfer was even more efficient than in native PCP (19). This effect was confirmed to occur also at 10 K (33). Although these PCP complexes were reconstituted with a single Chl species, Miller et al. have also demonstrated that reconstitution of PCP with a mixture of two Chl species produces PCP complexes having different Chl species in the two domains of the PCP monomer (32). The existence of PCP monomers with mixed Chl sites was confirmed by measurements of fluorescence and fluorescence excitation spectra (32), as well as by single molecule spectroscopy (24,34,35).

Here we further develop the single molecule spectroscopy studies by directly monitoring the interdomain Chl-Chl energy transfer in the PCP complexes reconstituted with a mixture of Chl species using femtosecond transient absorption spectroscopy. The observation of energy transfer unequivocally proves the existence of the PCP complexes with mixed Chl sites. Modeling the obtained energy transfer rates by the Förster equation provides further evidence for the Förster mechanism of energy transfer between Chl molecules located in different domains of monomeric PCP.

MATERIALS AND METHODS

Sample preparation

PCP was reconstituted from heterologously expressed N-domain apoprotein and purified pigments as described in Miller et al. (32). Before experiments, the samples were stored in the dark at 4°C. The optical density of the samples was adjusted by adding a buffer (25 mM Tris pH 7.5, 2 mM KCl) to yield optical density of at least 0.05 at the Q_y band maximum in a 2 mm cuvette. For fluorescence and fluorescence excitation measurements, a 1-cm path length quartz cuvette was used and the optical density of the samples was kept below 0.1 OD/cm.

Spectroscopic measurements

Steady-state absorption measurements were performed on a Jasco-V-530 (Easton, MD) spectrophotometer in a 2-mm path length quartz cuvette. Fluorescence and fluorescence excitation spectra were recorded using a Spex Flurolog (HORRIBA Jobin Yvon, Edison, NJ) fluorimeter. Femtosecond measurements were carried out using a femtosecond transient absorption spectrometer described elsewhere (19). The excitation pulses were obtained from pumping an optical parametric amplifier by 800-nm, 130-fs pulses generated in a regenerative amplifier; the probing pulses were generated by focusing a fraction of the regenerative amplifier output into a 0.3 cm sapphire plate. The mutual polarization of the pump and probe beams was set to the magic angle (54.7°). For signal detection, the probe beam and an identical reference beam (that had no overlap with the pump beam) were focused onto the entrance slit of a spectrograph, which then dispersed both beams onto a home-built dual photodiode array detection system. A 2-mm path length quartz rotating cuvette spinning at a rate ensuring that each excitation pulse hits a fresh sample was used to prevent degradation of the sample. Absorption spectra were measured before and after measurements to ensure that no permanent photochemical changes occurred over the duration of the experiment.

Analysis of time resolved spectra

All kinetic traces collected by the diode-array detection system were fitted globally. The data were fitted to a sum of exponentials, including numerical deconvolution of the full width at half-maximum (FWHM) of the response function, and a fourth degree polynomial describing the chirp. The fitting procedure used general linear regression for the amplitudes of the exponentials and the Nelder-Mead simplex method for the rate constants, the FWHM, and the chirp polynomial. To visualize the excited state dynamics, we used a model with time evolution according to a sequential, irreversible scheme A $\rightarrow$ B, B $\rightarrow$ C... The arrows represent increasingly slower monoexponential processes and the time constants of these processes correspond to lifetimes of the species A, B, C... The spectral profiles of the species are called evolution-associated difference spectra (EADS). In complex systems, EADS do not necessarily correspond to difference absorption spectra of particular excited states (36), so we have also applied target analysis for fitting the data obtained after peridinin excitation. For the target analysis, the data were chirp-corrected before the fitting procedure using the chirp polynomial obtained from the global fitting. The rate constants of the target analysis were fitted using the Nelder-Mead simplex method. General linear regression was used to obtain difference spectra of the individual excited states in the target analysis. In accordance with the terminology used by van Stokkum et al. (36), the difference spectra of the time components resulting from target analysis are called species-associated difference spectra (SADS).

RESULTS

Absorption spectra of the PCP complexes reconstituted with either Chl*b*/Chl*d* or Chl*a*/BChl*a* mixtures normalized to the peridinin absorption at 535 nm are shown in Fig. 1. The reconstituted PCP complexes have chlorophyll Q_y bands located at 650 nm and 700 nm (Chl*b*/Chl*d* mixture), and 672 nm and 790 nm (Chl*a*/BChl*a* mixture). The position of the Q_y

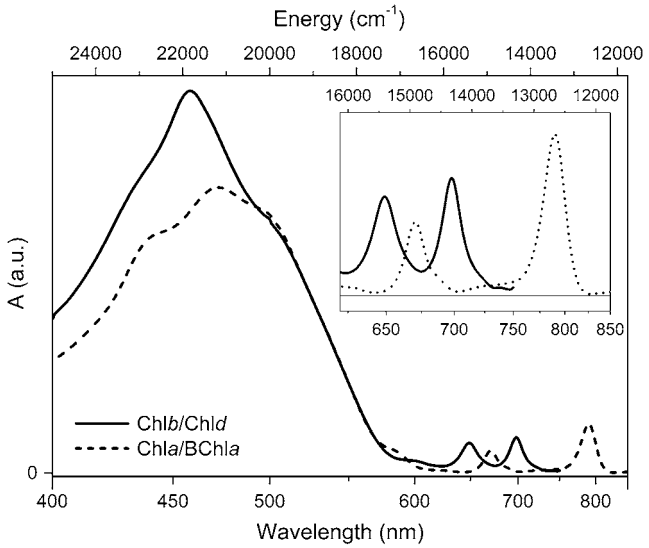

FIGURE 1 Absorption spectra of the reconstituted PCP complex with mixed Chl sites: Chl*b*/Chl*d* (*solid line*) AND Chl*a*/BChl*a* (*dashed line*). Spectra are normalized to peridinin absorption at 530 nm. (*Inset*) enlargement of the Q_y region of chlorophylls.

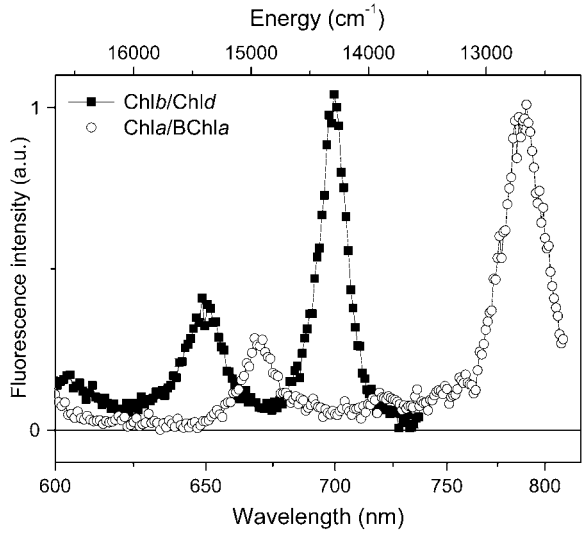

FIGURE 2 Fluorescence excitation spectra of the PCP complexes reconstituted with Chl*b*/Chl*d* (*solid symbols*) and Chl*a*/BChl*a* (*open symbols*) mixtures. Detection wavelengths were 740 nm (Chl*b*/Chl*d*) and 815 nm (Chl*a*/BChl*a*).

bands is identical to that observed for PCP complexes reconstituted with a single chlorophyll species (19,32,33), demonstrating successful incorporation of different chlorophyll species. The existence of PCP complexes that have different chlorophyll species in each domain of the monomer is demonstrated by fluorescence excitation spectra shown in Fig. 2. When emission is detected in the spectral region of emission of the chlorophyll with lower energy, at 740 nm for Chl*b*/Chl*d* mixture and at 815 nm for Chl*a*/BChl*a* mixture, the fluorescence excitation spectra contain a contribution from the chlorophyll lying at higher energy, due to energy transfer between the two chlorophyll species.

The Chl-Chl energy transfer is further corroborated by time-resolved experiments. In Fig. 3, transient absorption spectra recorded for the Chl*b*/Chl*d* mixture are shown at different time delays after excitation of Chl*b* at 650 nm. At 0.5 ps after excitation, the transient absorption spectrum exhibits two distinct bleaching bands at 650 nm (Chl*b*) and 700 nm (Chl*d*). The presence of Chl*d* bleaching is due to a direct excitation of Chl*d* that has a pronounced vibrational band overlapping with the Q_y band of Chl*b* (Supplementary Material, Fig. S1). At longer delays, there is a clear evidence of Chl*b*-Chl*d* energy transfer as decay of the Chl*b* bleaching is accompanied by a rise of the Chl*d* bleaching signal. In addition, the Chl*b* decay can be also followed in the excited state absorption (ESA) signal in the 570–610 nm region where Chl*b* ESA is markedly stronger than that of Chl*d*. This evolution is finished after ~200 ps (see kinetics in the *inset* of Fig. 3). The final transient absorption spectrum taken at 300 ps does not decay within the time window of the experiment because of the nanosecond lifetime of the terminal acceptor (37,38). The final spectrum also contains a contribution from Chl*b* as reconstitution of PCP with different chlorophyll species produces three classes of complexes composed of Chl*b*/Chl*b*, Chl*d*/Chl*d*, and Chl*b*/Chl*d* monomers ((24,32); see Discussion section for analysis of stoichiometric ratio). Consequently, excitation at 650 nm inevitably excites also PCP complexes with Chl*b*/Chl*b* composition. Since these cannot transfer energy to Chl*d*, they are the source of the residual Chl*b* bleaching signal at 300 ps (see Discussion section for further analysis).

Transient absorption spectra recorded for the Chl*a*/BChl*a* mixture after excitation of Chl*a* at 670 nm are shown in Fig. 4. The time evolution of the spectra is comparable with the Chl*b*/Chl*d* case, though the larger energy separation between the Q_y bands prevents direct excitation of BChl*a* at 670 nm, resulting in almost no BChl*a* signal in the transient absorption spectrum recorded at 0.5 ps after excitation. Energy transfer from Chl*a* to Bchl*a* is also manifested at 580 nm where BChl*a* Q_x bleaching grows in simultaneously with the BChl*a* Q_y bleaching at 790 nm.

To extract the time constants associated with Chl-Chl energy transfer, we have applied a global fitting analysis. We have excluded the data at time delays $<$300 fs, because these fast dynamics are due solely to relaxation within the excited state manifold of one chlorophyll species and do not contribute to Chl-Chl energy transfer. Under this approximation, fitting to a single-exponential function was sufficient to obtain good fits for both Chl*b*/Chl*d* and Chl*a*/BChl*a* PCP complexes. The resulting EADS are shown in Fig. 5. For the PCP complex containing the Chl*b*/Ch*d* mixture, the initial EADS has a contribution from both Chl*b* and Chl*d* Q_y bleaching. This EADS decays in 40 $\pm$ 5 ps to form the final, nondecaying spectrum characterized by the residual Chl*b*

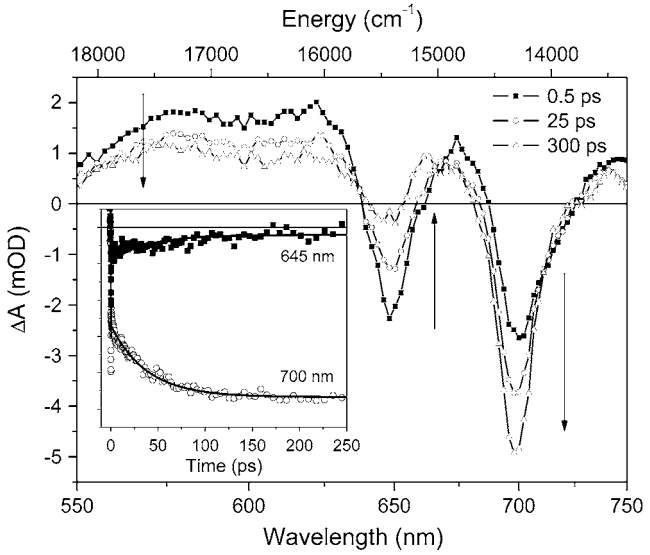

FIGURE 3 Transient absorption spectra recorded at different delays after 650 nm excitation of the PCP complex reconstituted with a Chl*b*/Chl*d* mixture. Arrows denote time evolution of the spectral features. (Inset) Kinetics measured at 645 nm (*solid symbols*) and 700 nm (*open symbols*). Solid lines represent fits.

bleaching and increased Chl*d* bleaching as a result of Chl*b*-Chl*d* energy transfer. Comparable results were obtained for the PCP complex with Chl*a*/BChl*a* mixture (Fig. 5), but the time constant of energy transfer is slower at 59 ± 3 ps.

For the PCP complex reconstituted with Chl*a*/BChl*a* mixture, we have also studied peridinin-Chl energy transfer

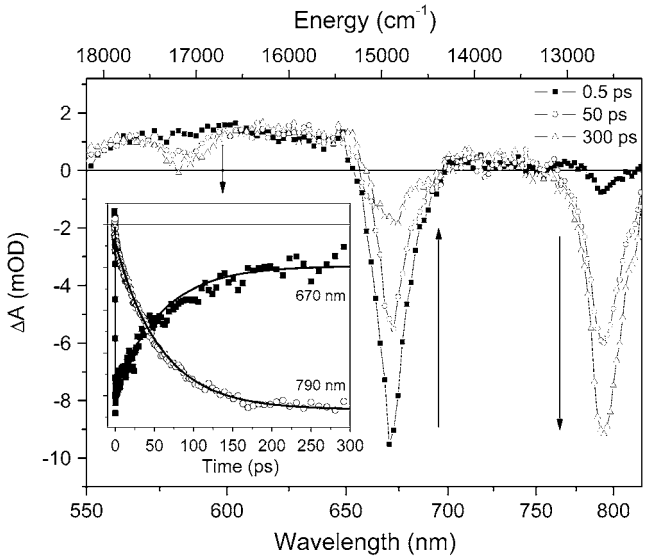

FIGURE 4 Transient absorption spectra recorded at different delays after 670 nm excitation of the PCP complex reconstituted with a Chl*a*/BChl*a* mixture. Arrows denote time evolution of the spectral features. (*Inset*) Kinetics measured at 675 nm (*solid symbols*) and 790 nm (*open symbols*). Solid lines represent fits.

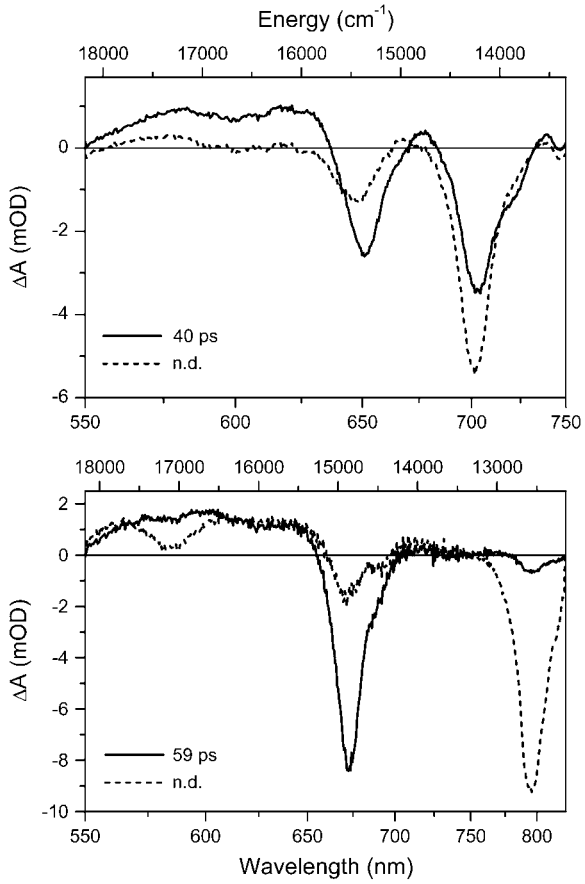

FIGURE 5 EADS resulting from global fitting of data obtained for PCP complexes reconstituted with Chl*b*/Chl*d* (*top*) and Chl*a*/BChl*a* mixtures (*bottom*). n.d., nondecaying component.

after excitation of peridinin at 510 nm (Fig. 6). At subpicosecond time delays, the spectra are dominated by a broad peridinin S_1/ICT ESA extending from 550 to 750 nm (8,10,19). However, even at 0.2 ps after excitation, there are obvious dips in the ESA spectrum located at 670 and 790 nm due to the bleaching of the Q_y bands of Chl*a* and BChl*a*, consistent with an ultrafast energy transfer channel via the peridinin S_2 state. This S_2 channel was found to operate with an efficiency in the range of 25–50% in both native (10–12) and reconstituted PCP complexes (19,33). Decay of the peridinin ESA, accompanied by a concomitant rise of both Chl*a* and BChl*a* bleaching, monitors energy transfer between peridinin and Chl*a*/BChl*a*. Kinetics recorded at maxima of the corresponding Q_y bleaching bands reveal that the peridinin-BChl*a* energy transfer is faster than the peridinin-Chl*a* energy transfer, in accordance with the results obtained for PCP complexes reconstituted with a single chlorophyll species (19). Peridinin-excited state spectral features have essentially disappeared in the transient absorption spectrum recorded at 5 ps, but further spectral evolution is observed in the Chl*a*/BChl*a* bleaching bands as a result of Chl*a*-BChl*a* energy transfer (Fig. 6).

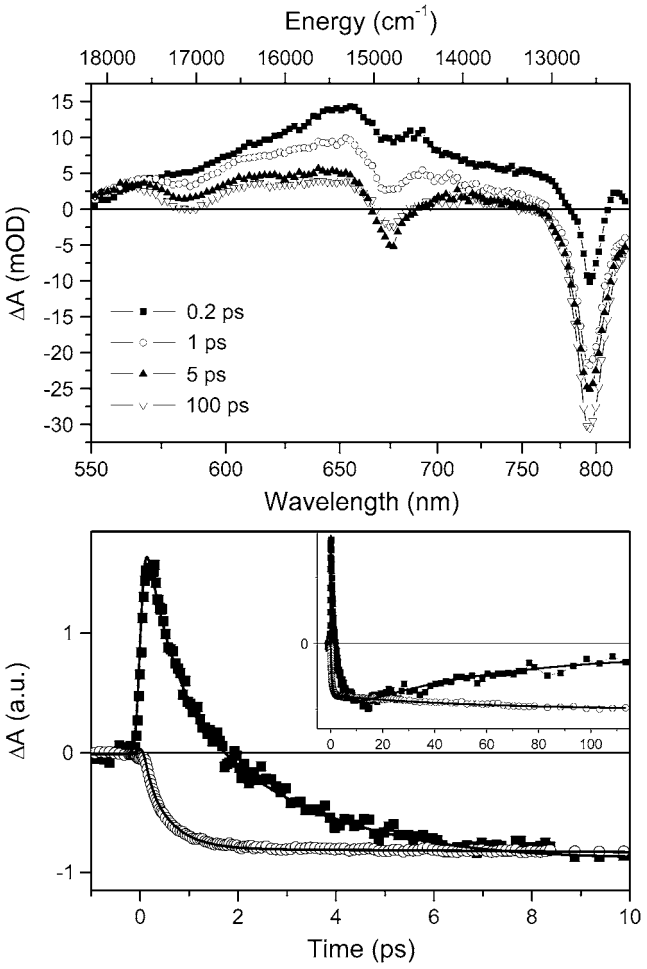

FIGURE 6 (*Top*) Transient absorption spectra measured after excitation of peridinin at 510 nm for the PCP complex reconstituted with a mixture of Chl*a* and BChl*a*. (*Bottom*) Kinetics recorded at 672 nm (Chl*a* bleaching, *solid symbols*) and 790 nm (BChl*a* bleaching, *open symbols*) normalized to minimum at 10 ps. Inset shows the time evolution of the bleaching signals at a longer timescale that reflects energy transfer between the two chlorophyll species. Solid lines are fits.

The EADS obtained from global fitting are shown in Fig. 7. The first EADS corresponds to the excited state species formed by ultrafast decay of the initially excited peridinin S_2 state. It has a characteristic shape of the peridinin S_1/ICT-S_N transition with Q_y bands superimposed on the broad ESA feature. From the magnitude of the Q_y bleaching, it may be deduced that the S_2 channel is more efficient with BChl*a* as the acceptor. This species decays in 0.5 ± 0.1 ps into the second EADS characterized by a large BChl*a* bleaching, whereas the magnitude of the Chl*a* bleaching band at 670 nm remains nearly the same as in the previous EADS. Further evolution (from *dashed* to *dotted* spectrum in Fig. 7) occurs with a 2.9 ± 0.3 ps time constant. The major change is deepening of the Chl*a* bleaching band at 670 nm accompanied by decay of the peridinin ESA, whereas no change is observed for the BChl*a* bleaching band at 790 nm. Consequently, the changes observed during these two steps are

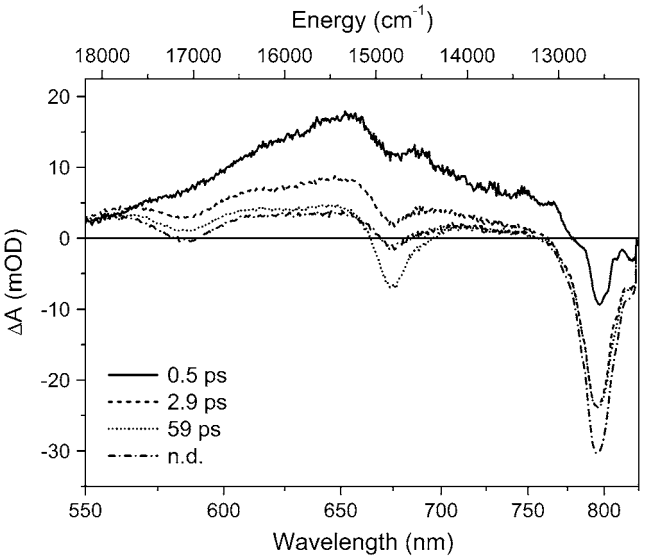

FIGURE 7 EADS resulting from global fitting of the data obtained after peridinin excitation (510 nm) of the PCP complex reconstituted with Chl*a*/BChl*a* mixture. Lifetimes of the individual excited state species are indicated. n.d., nondecaying component.

consistent with peridinin-BChl*a* and peridinin-Chl*a* energy transfer. The extracted time constants of 0.5 and 2.9 ps are in good agreement with those obtained for PCP complexes reconstituted with a single chlorophyll species (19). The last evolution step characterizes the Chl*a*-BChl*a* energy transfer. The time constant of this step, 59 ps, was extracted from the data obtained after direct excitation of Chl*a* (see above), and was therefore fixed during the fitting procedure.

DISCUSSION

The data presented in the previous section prove that the reconstitution of PCP with two chlorophyll species produces complexes having different chlorophylls in each of the two domains of the PCP monomer, confirming the initial fluorescence data (32) and recent single-molecular spectroscopy experiments (24,35,38). However, it is important to realize that the PCP complexes resulting from reconstitution with chlorophyll mixtures follow a statistical distribution. The bulk sample necessarily consists of three different classes of complexes: 1), those with one chlorophyll species in both domains, 2), those with the other chlorophyll species in both domains, and 3), those with different chlorophyll species in each domain. Statistical distribution of these three classes depends on the total ratio between the two chlorophyll species that can be deduced from magnitudes of the Q_y bands in absorption spectra of the reconstituted PCP complexes.

For the PCP complex reconstituted with Chl*b*/Chl*d* mixture, the intensity ratio of the Q_y bands is 0.82 (Fig.1), whereas the corresponding ratio of ε_{max} in dichloromethane is 0.57 (Table 1). Though this may suggest significant predominance of Chl*b* over Chl*d*, the coincidence of the first

vibrational band of Chl*d* with the Q_y band of Chl*b* must be taken into account (Fig. S1). Thus, Chl*d* contributes by ~30% to total absorption at 650 nm. Consequently, for equimolar amount of Chl*b* and Chl*d*, the ratio of intensities of the Q_y bands should be 0.74. Comparing this number with the experimental value of 0.82, it is obvious that the Chl*b*/Chl*d* ratio in this PCP complex is close to 1, meaning that the bulk sample consists of Chl*b*/Chl*b*, Chl*b*/Chl*d*, and Chl*d*/Chl*d* PCP complexes in the ratio of 1:2:1.

A different situation occurs for the PCP complex reconstituted with the Chl*a*/BChl*a* mixture. The intensity ratio of the Q_y bands is in this case 0.46, despite the fact that both chlorophyll species have comparable extinction coefficients at Q_y maximum (Table 1). Since the contribution of BChl*a* to absorption at the wavelengths corresponding to the Q_y maximum of Chl*a* (670 nm) is <10% (Fig. S1), we conclude that the Chl*a*/BChl*a* ratio in this PCP complex is close to 0.5. The fact that there is twice as much of BChl*a* leads to a different distribution of PCP complexes in the bulk sample. In this case, the Chl*a*/Chl*a*, Chl*a*/BChl*a*, and BChl*a*/BChl*a* PCP complexes will have a stoichiometric ratio of 1:4:4.

The different stoichiometric ratios have also consequences for the transient absorption experiments. For the PCP complex reconstituted with the Chl*b*/Chl*d* mixture, the ratio of 1:2:1 implies that excitation at 650 nm affects Chl*b* molecules that occur in both Chl*b*/Chl*b* complexes (33% of the excited complexes) and Chl*b*/Chl*d* complexes (66%). Since only those excited Chl*b* molecules occurring in the mixed PCP complexes can transfer energy to Chl*d*, there should be a residual signal corresponding to the 33% of Chl*b* molecules located in Chl*b*/Chl*b* PCP complexes when the energy transfer is completed. Chl*b* bleaching at 300 ps remains at ~⅓ of its value at 0.5 ps (Fig. 3) confirming the stoichiometric ratio determined from the absorption spectra. Similar analysis can be carried out for the Chl*a*/BChl*a* PCP complex, in which excitation at 670 nm affects an ensemble containing only 20% of Chl*a*/Chl*a* complexes, whereas the remaining 80% is due to excitation of the mixed Chl*a*/BChl*a* complexes. Again, as can be readily deduced from Fig. 4, the residual Chl*a* bleaching signal at 300 ps is ~20% of the initial bleaching at 0.5 ps, which is the value expected for the stoichiometric ratio obtained from the absorption spectrum. Since the values of the residual bleaching signal correspond well to the stoichiometric ratio of the complexes that cannot transfer energy, it implies that all excited Chl*b* (Chl*a*) molecules located in the mixed complexes transfer energy with nearly 100% efficiency to Chl*d* (BChl*a*).

It is useful to compare the stoichiometric ratios with the recent study of binding affinities of different Chl types in PCP (39). Using different molar ratios of Chls for reconstitution, Brotosudarmo et al. showed that both Chl*b* and acetyl Chl*a* (acChl*a*) have a binding affinity roughly twice of that of Chl*a* (39). Because both Chl*b*/Chl*d* and Chl*a*/BChl*a* PCP complexes used here were reconstituted with equimolar ratios of Chls, the results obtained here show that Chl*d* has about the same binding affinity as Chl*b*, whereas BChl*a* has a binding affinity twice that of Chl*a*. Underlying this result is the assumption that the relative absorbances of different chlorophylls in reconstituted PCP are similar to those in organic solvent. This may not be the case for the Chl*a*/BChl*a* pair, because in the PCP complexes reconstituted with single chlorophylls, the peridinin/Q_y ratio is slightly higher for Chl*a* (19), indicating that the Q_y extinction coefficient of Chl*a* is less than that of BChl*a* in PCP. Consequently the relative binding of BChl*a* is probably less than twice that of Chl*a*. Nevertheless, combining our results and those of Brotosudarmo et al. (39), we conclude that all nonnative Chls used so far for the reconstitution of PCP complexes have a higher binding affinity than the native pigment, Chl*a*. The fact that Chl*d*, BChl*a*, and Chl*b* have polar substituents in either R_1 or R_2 position (Fig. S3) supports the conjecture of Brotosudarmo et al. that the increase in binding affinity is due to formation of a Per-Chl hydrogen bond via the polar substituents in R_1 or R_2 positions (39).

Energy transfer between chlorophylls

Since the reconstitution clearly produces a significant fraction of PCP complexes with mixed chlorophyll sites, it provides an ideal platform for testing the energy transfer

TABLE 1 Parameters and results of the Förster energy transfer rate calculation

	ν^*_{max} (cm^{-1})	Γ^* (cm^{-1})	$\varepsilon^\dagger$ ($M^{-1}.cm^{-1}$)	$\mu^\ddagger$ (Debye)	κ/R^3 (nm^{-3})	$V^\P$ (cm^{-1})	$\Theta^\parallel$	τ^{**}_{ET} (ps)
Chl*b*	15410	445	56700	4.86	0.103[§]	9.5	2.604×10^{-4}	36
Chl*d*	14330	395	98900	6.27				(40)
Chl*a*	14930	375	89800	5.67		12.5	1.073×10^{-4}	50
BChl*a*	12660	460	96000	7.08				(59)

*Maxima and FWHM of the Q_y bands were obtained from fitting the Q_y bands in the PCP complexes reconstituted with Chl mixtures to a single Lorentzian profile.

†Values in dichloromethane, from Kobayashi et al. (46).

‡Transition dipole moments of the Q_y bands obtained from Eq. 4.

§Mean value taken from the range obtained from analysis of Kleima et al. (25).

¶Interaction term calculated from Eq. 3.

‖Overlap integral calculated from Eq. 2.

**Calculated energy transfer time, the experimental values are given in parentheses.

mechanism, because it allows tuning the spectral overlap between the donor and acceptor. It is generally accepted that Chl-Chl energy transfer in PCP proceeds via the Förster mechanism (25–27). Then, the energy transfer rate (in ps^{-1}) is calculated according to the following equation (40):

$$k_{ET} = 1.18V^2\Theta, \quad (1)$$

where V is the interaction term and Θ is the overlap integral.

The overlap integral Θ is calculated from the emission and absorption spectra of the donor and acceptor, $F(\nu)$ and $A(\nu)$:

$$\Theta = \int \frac{F(\nu)A(\nu)}{\nu^4} d\nu. \quad (2)$$

For the calculation, the absorption spectra $A(\nu)$ of the acceptor chlorophylls, Chl*d* and BChl*a*, were measured in acetone solution to avoid problems with the high energy tail of chlorophyll absorption overlapping with the onset of peridinin S_2 absorption in PCP. The resulting spectra were then shifted to match the Q_y absorption maximum in the reconstituted PCP complexes. The emission spectra of the donor chlorophylls, Chl*b* and Chl*a*, were taken from the fluorescence measurements on PCP complexes reconstituted with only Chl*b* or Chl*a* (Fig. S2). Before calculation of the spectral overlap, the fluorescence and absorption spectra, $F(\nu)$ and $A(\nu)$, were converted to the energy scale and normalized to unit area (40). Resulting values of Θ are listed in Table 1.

The interaction term, V, is calculated as

$$V = C\frac{5.04\mu_A\mu_D\kappa}{R^3}, \quad (3)$$

where μ_A and μ_D are transition dipole moments of the acceptor and donor, respectively, κ is the orientation factor, and R is the distance (in nanometers) between the centers of the transition dipole moment vectors of the donor and acceptor. C is a correction factor that takes into account effect of the medium, and for PCP has a value of 0.6 (41). The transition dipole moments were obtained from absorption spectra according to the equation (42)

$$\mu \approx 0.12\sqrt{\frac{\varepsilon_{max}\Gamma}{\nu_{max}}}, \quad (4)$$

where ε_{max} represents the extinction coefficient at the maximum of the Q_y band in $M^{-1}.cm^{-1}$ units, Γ is the FWHM of the Q_y band in cm^{-1}, and ν_{max} is the energy of the Q_y maximum in cm^{-1}. The published values of ε at Q_y maxima in dichloromethane were used for calculation, and Γ and ν_{max} were obtained from fitting the Q_y absorption bands in the reconstituted PCP complexes. All parameters used for calculation together with the resulting transition dipole moments are listed in Table 1.

The only remaining factors to calculate the Förster energy transfer rate are the orientation factor κ and the distance between the donor and acceptor chlorophylls, R. Assuming that the transition dipole moment of the Q_y band is oriented parallel with the y axis of the molecular frame of the chlorophyll molecule, these values can be readily obtained from the known PCP structure. However, as shown by van Zandvoort et al., the direction of the transition dipole moment of Q_y band may slightly deviate from the y axis (43). On the basis of the fluorescence anisotropy measurements on native PCP complex, Kleima et al. determined the range of possible angles between the Q_y transition dipole moment and y axis for Chl*a* molecules in PCP (2–7°), and calculated the corresponding range of κ/R^3 values to be 0.092–0.114 nm^{-3} (25). The mean value obtained from this range was used to calculate the Förster energy transfer rate in the reconstituted PCP complexes studied here.

The calculation of the Förster energy transfer rate from the values described above (also summarized in Table 1) yields the rates of 0.0275 ps^{-1} for the PCP complex reconstituted with the Chl*b*/Chl*d* mixture, and of 0.02 ps^{-1} for the Chl*a*/BChl*a* PCP complex. These values correspond to the energy transfer times of 36 ps (Chl*b*/Chl*d*) and 50 ps (Chl*a*/BChl*a*), matching well the values obtained from experiment, 40 and 59 ps, respectively, confirming that energy transfer between chlorophylls in the PCP monomer occurs via the Förster mechanism. The key factor playing a role upon chlorophyll exchange is the spectral overlap between the donor and acceptor. In the case of two Chl*a* molecules occurring in the native PCP complex, the ideal value of the spectral overlap gives the Chl-Chl energy transfer time of ~6 ps (25,26). When the energy gap between the donor emission and acceptor absorption increases to >100 nm, as in the case of the Chl*a*/BChl*a* PCP complex, the energy transfer slows down by an order of magnitude. Yet, given the 4 ns Chl*a* lifetime in the PCP complex (37,38), the Chl*a*-BChl*a* energy transfer in the reconstituted PCP complex is essentially 100% efficient. We have also calculated the spectral overlap for reverse (uphill) energy transfer. For the Chl*b*/Chl*d* pair, the spectral overlap between Chl*d* emission and Chl*b* absorption is about an order of magnitude lower than that for the downhill energy transfer, suggesting that contribution from back (Chl*d* to Chl*b*) energy transfer is <10%. In the case of the Chl*a*/BChl*a* pair, the back transfer is essentially impossible as the spectral overlap is $<10^{-6}$, resulting in values of energy transfer time longer than 1.5 ns.

It is interesting to compare the energy transfer rate obtained for the PCP complex reconstituted with the Chl*a*/BChl*a* mixture with that of the LH2 complex from *Rhodopseudomonas acidophila*, in which the B800 BChl*a* was replaced by Chl*a* (30). In both systems, the distance between donor (Chl*a*) and acceptor (BChl*a*) is nearly identical: 17.4 Å in PCP (9) and 17.7 Å in LH2 (4). Although the orientation factor κ is smaller for LH2, it is compensated by a larger value of the transition dipole moment of BChl*a* in LH2, leading to very similar calculated energy transfer times of 50 ps in PCP and 45 ps in LH2 (30). Although the experimentally obtained value matches the calculated one for the PCP

complex, the experiments carried out with the reconstituted LH2 complex gave Chl*a*-BChl*a* energy transfer time of 8.3 ps, about five times faster than expected from calculation (30). This discrepancy stems from the fact that whereas in PCP we deal with energy transfer between two monomeric chlorophylls, in LH2 the energy acceptor is formed by the excitonically coupled BChl*a* molecules (4). Thus, whereas the donor-acceptor pair in PCP fulfills all the conditions necessary for successful application of the standard Förster theory, to reproduce the energy transfer rate in LH2, it is necessary to apply a modified, multichromophoric Förster theory that accounts for the excitonic character of the acceptor (44,45).

Carotenoid-Chl energy transfer

The time constants of peridinin-Chl transfer for the Chla/BChla PCP complex yields 0.5 ps for the peridinin-BChla and 2.9 ps for the peridinin-Chla energy transfer. Since these values match well those obtained from earlier experiments with PCP complexes reconstituted with a single chlorophyll (19), it is obvious that presence of two different chlorophyll species in the PCP monomer does not affect peridinin-Chl transfer. Yet, the sequential fitting model used to obtain these time constants is, due to three different types of complexes presented in the bulk sample, only an approximation, and the individual EADS shown in Fig. 7 does not represent pure excited state species. Therefore, we have applied a target analysis that fits the data to a model shown in Fig. 8. In this model, we denote the absorbing state of peridinin S_2 if it occurs in the domain containing Chl*a*, and S_2' if it contains BChl*a*. Accordingly, the S_1/ICT and S_1/ICT′ denotes the lowest excited states of peridinin associated with Chl*a* and BChl*a*, respectively. We assume that there is no S_2-S_2' or S_1/ICT-S_1/ICT′ energy transfer and that the transient absorption spectra of the S_1/ICT and S_1/ICT′ are identical. This assumption is justified because no change in the shape of the S_1/ICT transient spectrum was found upon the change of chlorophyll species in the PCP complexes reconstituted with a single chlorophyll species (19). The Chl*a*-BChl*a* energy transfer component was fixed to 59 ps, the value obtained from direct excitation of Chl*a*. The resulting SADS corresponding to the S_1/ICT, Chl*a*, and BChl*a* excited state species are shown in Fig. 8. The time constants for the S_1/ICT and S_1/ICT′ lifetimes are now 2.25 ps and 0.4 ps. Assuming the intrinsic S_1/ICT lifetime of 16 ps (11), these values give energy transfer times of 2.6 ps and 0.41 ps, corresponding to the efficiencies of the S_1/ICT pathway of 86 and 98% for the peridinin-Chl*a* and peridinin-BChl*a* energy transfer.

SUMMARY

Time-resolved measurements of PCP reconstituted with a mixture of two different Chl species proved that this reconstitution produced PCP complexes with mixed chlorophyll

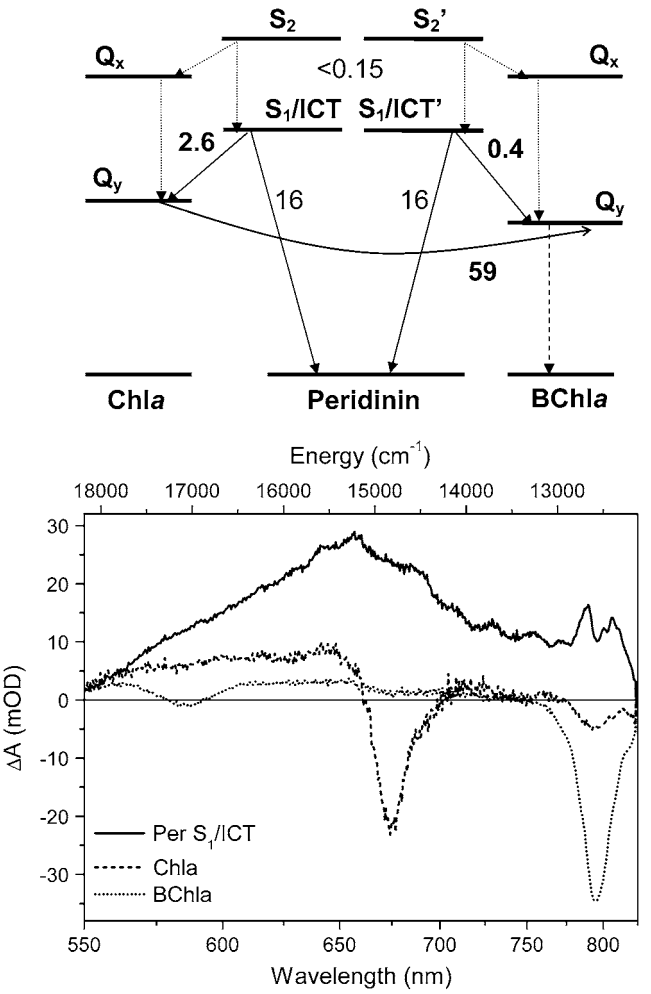

FIGURE 8 Model (*top*) and results (*bottom*) of the target analysis applied to data measured after excitation of peridinin into the S_2 state at 510 nm for the PCP complex reconstituted with Chl*a*/BChl*a* mixture. The S_2' and S_1/ICT′ states refer to peridinin molecules associated with BChl*a*, the S_2, and S_1/ICT to those associated with Chl*a*. The major energy transfer channels are depicted by solid arrows, and each channel is labeled by a time constant in picoseconds. The ultrafast channels that could not be resolved in the target analysis due to limited time resolution are depicted by dotted arrows. The <0.15 ps time constant refers to depopulation of the peridinin S_2 state. The fluorescence from the final state (Bchl*a* Q_y state) is shown as a dashed arrow. The bottom panel shows the resulting SADS.

sites and allowed direct monitoring of energy transfer between the two Chl species. Analysis of absorption and transient absorption spectra revealed another interesting property of the Chl binding site in PCP. Comparison of our time-resolved measurements with steady-state absorption data (39) clearly suggests that the binding site has lowest affinity for Chl*a*, the pigment occurring in the native PCP complex. Energy transfer rates modeled by the Förster equation match those obtained from experiment, confirming the Förster mechanism suggested earlier for native PCP (25). This result demonstrates robustness of the light-harvesting strategy of PCP. Refolding the protein with different pigments and

introducing asymmetry in Chl binding sites does not affect the structural features of the complex and maintains the highly efficient energy transfer pathways of the native complex. For peridinin-Chl transfer, the efficiency of the reconstituted PCP can be even higher than in the native complex; in the Chl*a*/BChl*a* system, BChl*a* is a ''faster'' acceptor than native Chl*a*. Reconstituted PCP complexes are an ideal tool for studies of energy transfer pathways such as the yet-unclear peridinin-Chl S_2-Q_x pathway (10–12,19). Similarly, the BChl*a* reconstitution provides a perfect platform for experimental search of the so-called blue peridinin in PCP (17), because the Soret band of BChl*a* does not overlap with the peridinin absorption. Reconstituted PCP complexes may also serve as model systems for designing artificial antenna. Recently peridinin and related carotenoids have been used in artificial systems, in which their specific excited state properties allowed for tuning energy transfer efficiency by varying solvent polarity (22).

SUPPLEMENTARY MATERIAL

To view all of the supplemental files associated with this article, visit www.biophysj.org.

The authors thank Harry A. Frank for useful and stimulating discussions, Frank Sharples for maintaining the algal cultures, and Min Chen for *Acaryochloris* cells.

T.Po. thanks the Swedish Energy Agency for supporting his stay in Sweden, and the Czech Ministry of Education (grants No. MSM6007665808 and AV0Z50510513) and the Grant Agency of the Czech Academy of Sciences (IAA608170604) for supporting his research in the Czech Republic. The work at Lund University was supported by grants from the Swedish Research Council and the Wallenberg Foundation.

REFERENCES

1. Green, R. B., and W. W. Parson, editors. 2003. Light-Harvesting Antennas in Photosynthesis. Kluwer, Dordrecht, The Netherlands.
2. MacColl, R., and D. Guard-Friar. 1987. Phycobiliproteins. CRC Press, Boca Raton.
3. Polívka, T., and V. Sundström. 2004. Ultrafast dynamics of carotenoid excited states—from solution to natural and artificial systems. *Chem. Rev.* 104:2021–2071.
4. Sundström, V., T. Pullerits, and R. van Grondelle. 1997. Photosynthetic light-harvesting: reconciling dynamics and structure of purple bacterial LH2 reveals function of photosynthetic unit. *J. Phys. Chem. B.* 103:2327–2346.
5. Ritz, T., A. Damjanovic, K. Schulten, J. P. Zhang, and Y. Koyama. 2000. Efficient light harvesting through carotenoids. *Photosynth. Res.* 66:125–144.
6. van Amerongen, H., and R. van Grondelle. 2001. Understanding the energy transfer function of LHCII, the major light-harvesting complex of green plants. *J. Phys. Chem. B.* 105:604–617.
7. Bautista, J. A., R. G. Hiller, F. P. Sharples, D. Gosztola, M. R. Wasielewski, and H. A. Frank. 1999. Singlet and triplet energy transfer in the peridinin-chlorophyll a protein from *Amphidinium carterae*. *J. Phys. Chem. A.* 103:2267–2273.
8. Polívka, T., R. G. Hiller, and H. A. Frank. 2007. Spectroscopy of the peridinin-chlorophyll-a protein: insight into light-harvesting strategy of marine algae. *Arch. Biochem. Biophys.* 458:111–120.
9. Hofmann, E., P. M. Wrench, F. P. Sharples, R. G. Hiller, W. Welte, and K. Diederichs. 1996. Structural basis of light harvesting by carotenoids: peridinin-chlorophyll-protein from *Amphidinium carterae*. *Science.* 272:1788–1791.
10. Krueger, B. P., S. S. Lampoura, I. H. M. van Stokkum, E. Papagiannakis, J. M. Salverda, C. C. Gradinaru, D. Rutkauskas, R. G. Hiller, and R. van Grondelle. 2001. Energy transfer in the peridinin chlorophyll—a protein of *Amphidinium carterae* studied by polarized transient absorption and target analysis. *Biophys. J.* 80:2843–2855.
11. Zigmantas, D., R. G. Hiller, V. Sundstrom, and T. Polívka. 2002. Carotenoid to chlorophyll energy transfer in the peridinin-chlorophyll-a-protein complex involves an intramolecular charge transfer state. *Proc. Natl. Acad. Sci. USA.* 99:16760–16765.
12. Linden, P. A., J. Zimmermann, T. Brixner, N. E. Holt, H. M. Vaswani, R. G. Hiller, and G. R. Fleming. 2004. Transient absorption study of peridinin and peridinin-chlorophyll-a-protein after two photon excitation. *J. Phys. Chem. B.* 108:10340–10345.
13. Bautista, J. A., R. E. Connors, B. B. Raju, R. G. Hiller, F. P. Sharples, D. Gosztola, M. R. Wasielewski, and H. A. Frank. 1999. Excited state properties of peridinin: observation of a solvent dependence of the lowest excited singlet state lifetime and spectral behavior unique among carotenoids. *J. Phys. Chem. B.* 103:8751–8758.
14. Frank, H. A., J. A. Bautista, J. Josue, Z. Pendon, R. G. Hiller, F. P. Sharples, D. Gosztola, and M. R. Wasielewski. 2000. Effect of the solvent environment on the spectroscopic properties and dynamics of the lowest excited states of carotenoids. *J. Phys. Chem. B.* 104:4569–4577.
15. Zigmantas, D. R. G., F. P. Hiller, H. A. Sharples, V. Frank, V. Sundström, and T. Polívka. 2004. Effect of a conjugated carbonyl group on the photophysical properties of carotenoids. *Phys. Chem. Chem. Phys.* 6:3009–3016.
16. Vaswani, H. M., C. P. Hsu, M. Head-Gordon, and G. R. Fleming. 2003. Quantum chemical evidence for an intramolecular charge-transfer state in the carotenoid peridinin of peridinin-chlorophyll-protein. *J. Phys. Chem. B.* 107:7940–7946.
17. Shima, S., R. P. Ilagan, N. Gillespie, B. J. Sommer, R. G. Hiller, F. P. Sharples, H. A. Frank, and R. R. Birge. 2003. Two-photon and fluorescence spectroscopy and the effect of environment on the photochemical properties of peridinin in solution and in the peridinin-chlorophyll-protein from *Amphidinium carterae*. *J. Phys. Chem. B.* 107: 8052–8066.
18. Papagiannakis, E., D. S. Larsen, I. H. M. van Stokkum, M. Vengris, R. G. Hiller, and R. van Grondelle. 2004. Resolving the excited state equilibrium of peridinin in solution. *Biochemistry.* 43:15303–15309.
19. Polívka, T., T. Pascher, V. Sundström, and R. G. Hiller. 2005. Tuning energy transfer in the peridinin-chlorophyll complex by reconstitution with different chlorophylls. *Photosynth. Res.* 86:217–227.
20. Polívka, T., I. H. M. van Stokkum, D. Zigmantas, R. van Grondelle, V. Sundström, and R. G. Hiller. 2006. Energy transfer in the major intrinsic light-harvesting complex from *Amphidinium carterae*. *Biochemistry.* 45:8516–8526.
21. Papagiannakis, E., I. H. M. van Stokkum, H. Fey, C. Büchel, and R. van Grondelle. 2005. Spectroscopic characterization of the excitation energy transfer in the fucoxanthin-chlorophyll protein of diatoms. *Photosynth. Res.* 86:241–250.
22. Polívka, T., M. Pellnor, E. Melo, T. Pascher, V. Sundström, A. Osuka, and K. R. Naqvi. 2007. Polarity-tuned energy transfer efficiency in artificial light-harvesting antennae containing carbonyl carotenoids peridinin and fucoxanthin. *J. Phys. Chem. C.* 111:467–476.
23. Krikunova, M., H. Lokstein, D. Leupold, R. G. Hiller, and B. Voigt. 2006. Pigment-pigment interactions in PCP of *Amphidinium carterae* investigated by nonlinear polarization spectroscopy in the frequency domain. *Biophys. J.* 90:261–271.
24. Wörmke, S., S. Mackowski, T. H. P. Brotosudarmo, C. Jung, A. Zumbusch, M. Ehrl, H. Scheer, E. Hofmann, R. G. Hiller, and C. Bräuchle. 2007. Monitoring fluorescence of individual chromophores in peridinin-chlorophyll-protein complex using single molecule spectroscopy. *Biochim. Biophys. Acta.* 1767:956–964.

25. Kleima, F. J., E. Hofmann, B. Gobets, I. H. M. van Stokkum, R. van Grondelle, K. Diederichs, and H. van Amerongen. 2000. Förster excitation energy transfer in peridinin-chlorophyll-a-protein. *Biophys. J.* 78:344–353.

26. Ilagan, R. P., S. Shima, A. Melkozernov, S. Lin, R. E. Blankenship, F. P. Sharples, R. G. Hiller, R. R. Birge, and H. A. Frank. 2004. Spectroscopic properties of the main-form and high-salt peridinin-chlorophyll a proteins from *Amphidinium carterae*. *Biochemistry.* 43:1478–1487.

27. Ilagan, R. P., J. F. Koscielecki, R. G. Hiller, F. P. Sharples, G. N. Gibson, R. R. Birge, and H. A. Frank. 2006. Femtosecond time-resolved absorption spectroscopy of main-form and high-salt peridinin-chlorophyll-a proteins at low temperatures. *Biochemistry.* 45:14052–14063.

28. Reference deleted in proof.

29. Bandilla, M., B. Ucker, M. Ram, I. Simonin, E. Gelhaye, G. McDermott, R. J. Cogdell, and H. Scheer. 1998. Reconstitution of the B800 bacteriochlorophylls in the peripheral light harvesting complex B800–850 of *Rhodobacter sphaeroides* 2.4.1. with BChl a and modified (bacterio)chlorophylls. *Biochim. Biophys. Acta.* 1364:390–402.

30. Herek, J. L., N. J. Fraser, T. Pullerits, P. Martinsson, T. Polívka, H. Scheer, R. J. Cogdell, and V. Sundström. 2000. Mechanism of B800–B850 energy transfer in native and modified LH2 complexes of *Rps. acidophila* 10050. *Biophys. J.* 78:2590–2596.

31. Paulsen, H. 2006. Reconstitution and pigment exchange. *In* Chlorophylls and Bacteriochlorophylls: Biochemistry, Biophysics, Functions and Applications. B. Grimm, R. J. Porra, W. Rüdiger, and H. Scheer, editors. Springer, Dordrecht, The Netherlands. 375–385.

32. Miller, D. J., J. Catmull, R. Puskeiler, H. Tweedale, F. P. Sharples, and R. G. Hiller. 2005. Reconstitution of the peridinin chlorophyll a protein (PCP): evidence for functional flexibility in chlorophyll binding. *Photosynth. Res.* 86:229–240.

33. Ilagan, R. P., T. W. Chapp, R. G. Hiller, F. P. Sharples, T. Polívka, and H. A. Frank. 2006. Optical spectroscopic studies of light-harvesting by pigment-reconstituted peridinin-chlorophyll-proteins at cryogenic temperatures. *Photosynth. Res.* 90:5–15.

34. Brotosudarmo, T. H. P., E. Hofmann, R. G. Hiller, S. Wörmke, S. Mackowski, A. Zumbusch, C. Bräuchle, and H. Scheer. 2006. Peridinin-chlorophyll-protein reconstituted with chlorophyll mixtures: preparation, bulk and single molecule spectroscopy. *FEBS Lett.* 580:5257–5262.

35. Mackowski, S., S. Wörmke, T. H. P. Brotosudarmo, C. Jung, R. G. Hiller, H. Scheer, and C. Bräuchle. 2007. Energy transfer in reconstituted peridinin-chlorophyll protein complexes: ensemble and single molecule spectroscopy studies. *Biophys. J.* 93:3249–3258.

36. van Stokkum, I. H. M., D. S. Larsen, and R. van Grondelle. 2004. Global and target analysis of time-resolved spectra. *Biochim. Biophys. Acta.* 1657:82–104.

37. Koka, P., and P. S. Song. 1977. Chromophore topography and binding environment of peridinin-chlorophyll-a protein complexes from marine dinoflagellate algae. *Biochim. Biophys. Acta.* 495:220–231.

38. Mackowski, S., S. Wörmke, T. H. P. Brotosudarmo, H. Scheer, and C. Bräuchle. 2008. Fluorescence spectroscopy of reconstituted peridinin-chlorophyll protein complexes. *Photosynth. Res.* 95:253–260.

39. Brotosudarmo, T. H. P., S. Mackowski, E. Hofmann, R. G. Hiller, C. Bräuchle, and H. Scheer. 2008. Relative binding affinities of chlorophylls in peridinin-chlorophyll-protein reconstituted with heterochlorophyllous mixtures. *Photosynth. Res.* 95:247–252.

40. Pullerits, T., S. Hess, J. L. Herek, and V. Sundström. 1997. Temperature dependence of excitation transfer in LH2 of *Rhodobacter sphaeroides*. *J. Phys. Chem. B.* 101:10560–10567.

41. Kleima, F. J., M. Wendling, E. Hofman, E. J. G. Peterman, R. van Grondelle, and H. van Amerongen. 2000. Peridinin chlorophyll a protein: relating structure and steady-state spectroscopy. *Biochemistry.* 39:5184–5195.

42. Gilbert, A., and J. Baggott. 1991. Essentials of Molecular Photochemistry. Blackwell Science. Oxford.

43. van Zandvoort, M. A. M. J., D. Wrobel, P. Lettinga, G. van Ginkel, and Y. K. Levine. 1995. The orientation of the transition dipole moments of chlorophyll a and pheophytin a in their molecular frame. *Photochem. Photobiol.* 62:299–308.

44. Jang, S., M. D. Newton, and R. J. Silbey. 2007. Multichromophoric Förster resonance energy transfer from B800 to B850 in the light harvesting complex 2: evidence for subtle energetic optimization by purple bacteria. *J. Phys. Chem. B.* 111:6807–6814.

45. Kimura, A., and T. Kakitani. 2003. Theory of excitation energy transfer in the intermediate coupling case of clusters. *J. Phys. Chem. B.* 107: 14486–14499.

46. Kobayashi, M., M. Akiyama, H. Kano, and H. Kise. 2006. Spectroscopy and structure determination. *In* Chlorophylls and Bacteriochlorophylls: Biochemistry, Biophysics, Functions and Applications. B. Grimm, R. J. Porra, W. Rüdiger, and H. Scheer, editors. Springer, Dordrecht, The Netherlands. 79–94.